through the line-width regions as the temperature is lowered. The reappearance (or narrowing) of the methyl resonance at 77 K indicates the "long correlation" regime has been reached.[45] The methyl carbons in cured epoxy resins show a similar broadening as illustrated in Figure 2. In addition, this type of line-width effect has been reported in poly(tetrafluoroethylene)[33] at the onset of the rapid molecular reorientation about the chain axis which accompanies the 19 °C phase transition.

Although line-width contributions arising from motional effects can cause resolution problems in the solid-state experiments, line-width data as a function of temperature can provide a ready measure of rotational barriers. Using this type of analysis, Rothwell and Waugh[44] have determined the methyl rotational barrier in hexamethylethane, the hexad rotational barrier in hexamethylbenzene, and the rotational barrier in β-phase adamantane.

A similar broadening of resonance lines can occur when the molecular motion is comparable to the coherent motion introduced into the spin system by magic-angle spinning. Waugh et al.[46,47] have carried out line-width vs. temperature studies at different spinning rates on decamethylferrocene and hexamethylbenzene and have determined the barrier to the five-site jump process in the former and studied the 116 K phase transition in the latter. The importance of this type of experiment is that, in the limit of very slow spinning rates, detection of motional frequencies of a few hertz are possible.

Conclusions

The provision for VT-MAS extends the range of applications of CPMAS NMR to a broad spectrum of chemical areas including reactive species, unstable systems, and mechanisms of molecular reorientation. The initial results of variable-temperature CPMAS ^{13}C NMR studies have demonstrated considerable potential for elucidating structure and dynamics in the solid state.

(45) The authors thank Dr. Volker Macho, IBM San Jose, for obtaining the 77-K spectrum.

(46) D. Suwelack, W. P. Rothwell, and J. S. Waugh, *J. Chem. Phys.*, **73**, 2559 (1980).
(47) M. M. Maricq and J. S. Waugh, *J. Chem. Phys.*, **70**, 3300 (1979).

Mössbauer Effect Studies of Intercalation Compounds

ROLFE H. HERBER

Department of Chemistry, Rutgers University, New Brunswick, New Jersey 08903

Received June 15, 1981 (Revised Manuscript Received March 30, 1982)

Intercalation compounds[1] are formed from solids of low dimensionality in which there exists a large anisotropy in the chemical bonding forces. Such solids are characterized by layers of atoms held together by van der Waals type bonds. These layers can be pried apart by chemical means to effect the insertion of a "guest" species into the "host" lattice. The guest species may be either electron donors (alkali metals, alkaline earths, or rare earths), electron acceptors (AsF_5, SbF_5), or organic and inorganic molecules that can form weak bonds with the host matrix. Intercalation invariably results in significant modifications in the interlayer distance and can bring about pronounced changes in the properties of the host matrix, including changes in the electrical conductivity by many orders of magnitude,[2] an increase (or decrease) in the superconducting transition temperature of the matrix,[3] the specific heat and related properties of the solid,[4] the optical[5] and magnetic[6] properties of the layered material, and the structural properties of the system,[4,7] inter alia.

Rolfe H. Herber was born in Dortmund, Germany, in 1927 and came to the U.S. just prior to World War II. He received his B.S. at UCLA in 1949 and his Ph.D. at Oregon State University in 1952. After postdoctoral work at M.I.T., he was on the faculty of the University of Illinois before coming to Rutgers University in 1959. He has been a Senior N.S.F. Postdoctoral Fellow at the Weizmann Institute and Visting Senior Scientist at CENG, Grenoble, France. He is currently the Karl Taylor Compton Professor of Physics at the Technion-Israel Institute of Technology while on leave from Rutgers University. His research interests lie in the area of structural chemistry and solid-state physics.

Because of the range of chemical and physical properties influenced by intercalation, a large number of physicochemical techniques have been used to elucidate the intercalation process. Recently nuclear γ-ray resonance spectroscopy (the Mössbauer effect)[8] has joined this list, and a great deal of new information has been

(1) For a recent review, see Jean Rouxel in "Layered Materials and Intercalates"; van Bruggen, C. F., Haas, C., Myron, H. W., Eds.; North Holland: Amsterdam, 1980, pp 3–11.
(2) Kanamaru, F.; Shimada, M.; Koizumi, M.; Takada, T. *J. Solid State Chem.*, **1973**, *7*, 1. Kikkawa, S.; Fanamaru, F.; Koizumi, M. *Bull. Chem. Soc. Jpn.*; **1979**, *52*, 963.
(3) Whittingham, M. Stanley. *Progr. Solid State Chem.* **1978**, *12*, 41. Schollhorn, Robert; Lerf, Anton; Sernetz, Friedrich *Z. Naturorsch. B*, **1974**, *29B*, 810; *Mater. Res. Bull.*, **1974**, *9*, 1597.
(4) Meyer, S. F. Howard, R. E.; Stewart, G. R.; Acrivos, J. U.; Geballe, T. H. *J. Chem. Phys.*, **1975**, *62*, 441.
(5) Solin, S. A. *Physica B + C (Amsterdam)*, **1980**, *99*, 443; Nemanich, R. J.; Solin, S. A.; Guérard, D. *Phys. Rev. B*, **1977**, *16*, 2965. Underhill, C.; Leung, S. Y.; Dresselhaus, G.; Dresselhaus, M. S. *Solid State Commun.*, **1979**, *29*, 769.
(6) Halbert, Thomas R.; Johnston, D. C.; McCandlish, L.E; Thompson, A.H.; Scanlon, J. C.; Dumesic, J.A. *Pysica B + C (Amsterdam)*, **1980**, *99*, 128. Eibschutz, Marcu; DiSalvo, F. *Phys. Rev. Lett.* **1976**, *36*, 104. DiSalvo, Frank J. "Low Temperature Physics"; Timmerhaus, K.D., O'Sullivan, W.J., Hammel, E.F., Eds.; Plenum Press: New York, Vol. 3.
(7) Chianelli, R.R.; Scanlon, J.C.; Whittingham, M.S.; Gamble, F.R. *Inorg. Chem.*, **1975**, *14*, 1691. Gamble, R.R.; Osiecki, J.H.; DiSalvo, F.J. *J. Chem. Phys.* **1971**, *55*, 3525. G.A. Wiegers, *Physica B + C (Amsterdam)*, 1980, *99*, 151.
(8) See Chapter 15 in "Physical Methods in Chemistry", Drago, Russell S. W.B. Saunders: Philadelphia, 1977, and references therein. Herber, R.H. *J. Chem. Educ.*, **1965**, *42*, 180. "Topics In Applied Physics", Gonser, U., Ed.; Springer Verlag: New York, 1975, Vol. 5.

0001-4842/82/0115-0216$01.25/0

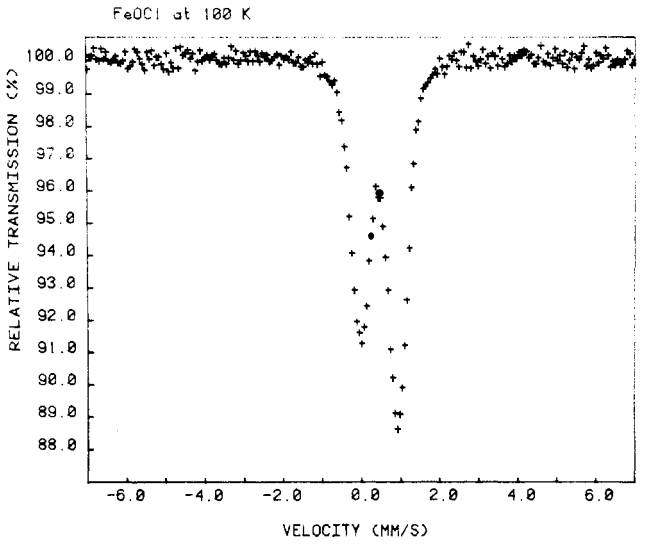

Figure 1. Mössbauer effect spectrum of FeOCl at 100 K. The two resonance maxima are separated by an energy corresponding to the quadrupole splitting (QS) parameter. The energy difference between the centroid of the spectrum and the horizontal axis reference point is the isomer shift (IS) parameter. The total area under the resonance curve (A) is related to the recoil-free fraction (f) of the ^{57}Fe nucleus.

extracted from such studies.

Mössbauer Parameters and Their Significance in the Study of Intercalates

In Mössbauer spectroscopy the interaction between an appropriate nucleus and its electronic environment is probed by carefully modulating the energy of the γ ray emitted by a suitable source. The effect of this modulation is observed by determining the change in the transmission of the γ radiation through the experimental sample of interest. Thus, a typical Mössbauer spectrum consists of a display of intensity of the transmitted radiation as a function of modulation energy. The latter is almost invariably expressed as a Doppler energy in units of mm s^{-1}.

A representative Mössbauer spectrum of an intercalation matrix—in this case the anisotropic layer compound FeOCl—is shown in Figure 1. Detailed examination of this figure shows that from such a spectrum, and others obtained at different temperatures, a number of parameters characteristic of the sample can be readily extracted. Among these are (a) the isomer shift (IS), (b) the quadrupole hyperfine interaction (QS), and (c) the area under the resonance curve (A). The IS arises from the interaction between the nucleus and the electrons surrounding it, and changes in the IS reflect primarily changes in the s-electron population, since it is only such electrons which have an appreciable density at the nucleus. In many instances the formal oxidation state (e.g., whether ferrous or ferric iron, stannous or stannic tin, etc.) and the spin state (e.g., whether high spin or low spin) can be determined from the absolute value of the IS parameter.[9,10] In addition, the temperature dependence of the isomer shift can provide information concerning the effective dynamical mass[11] of the Mössbauer active atom. This mass can, in turn, be related to the covalency of the bonding between the Mössbauer active atom and its nearest neighbor environment.

The QS parameter arises from the interaction between the nuclear quadrupole moment and the gradient of the electrostatic field at the nucleus. Most dramatically, for the Mössbauer nuclei ^{57}Fe, ^{119}Sn, and ^{197}Au, a cubic charge environment—as, for example, in octahedral or tetrahedral symmetry—leads to the observation of a single resonance maximum. On the other hand, when the charge symmetry is less than cubic, as, for example, in the case of the cis dichloro, tetraoxo, nearest-neighbor arrangement in FeOCl,[12,13] there are two resonance maxima in the spectrum,[14] as shown in Figure 1. The energy of separation of the two resonance lines is the nuclear quadrupole coupling and reflects the distortion of the electronic environment from cubic symmetry. The temperature dependence of the QS parameter can provide a sensitive measure of both changes in bond angles and distances with temperature and of the thermally driven population of various electronic sublevels of the Mössbauer active atom.

The area under the resonance curve is related not only to the number of resonant atoms of a given kind in the optical path of the experiment (and thus can provide clues about the relative numbers of chemically different atoms of the same element which are present) but also to the probability that a γ ray will be absorbed without recoil. This latter probability is called the recoil-free fraction, f. The temperature dependence of ln f, in turn, can be used to extract lattice dynamical information from a series of Mössbauer experiments. Most important among these are the lattice temperature, θ_M, as probed by the Mössbauer atom, and the anisotropy[15] in the vibrational amplitude, $\langle x^2 \rangle_{\parallel} - \langle x^2 \rangle_{\perp}$.

In addition to the above parameters, considerable other information relating to magnetic hyperfine interactions, crystallographic phase changes, and electronic sublevel degeneracies can be extracted from Mössbauer spectroscopic data. These will not be considered in the present discussion.

Studies of Guest Moieties

Sn. One of the first intercalation solids studied in detail in our laboratory by Mössbauer effect spectroscopy using the 23.8-keV radiation of ^{119m}Sn is the tin–tantalum sulfide system. TaS_2 can be prepared in several different polytypes,[16] of which the 2H form has been studied in considerable detail. 2H-TaS_2 is a superconductor with a T_c of 0.7 K.[17,18] There are two tin

(9) Dunlap, B.D.; Kalvius, G. M. in "Mössbauer Isomer Shifts", Shenoy, G.K., Wagner, F.E. Eds.; North Holland: Amsterdam, 1978, pp 15–48.

(10) For Fe and Ni, see Ingalls, Robert; van der Woude, F.; Sawatzky, G.A. in "Mössbauer Isomer Shifts", Shenoy, G.K., Wagner, F.E., Eds.; North Holland: Amsterdam, 1978, pp 361–429. For Sn, see Flinn, P.A. *ibid.*, pp 593–616. For Sb, Te, I, and Xe, see Ruby, S.L.; Shenoy, G.K. *ibid.*, pp 617–659.

(11) Pound, R.V.; Rebka, G.A. Jr., *Phys. Rev. Lett.*, **1960**, *4*, 274. Montano, P.A.; Seehra, M.S. *Phys. Rev. B* **1977**, *15*, 2437.

(12) Goldsztaub, S.A.; *C.R. Acad. Sci. Fr.*, **1934**, *198*, 667. *Bull. Soc. Fr., Mineral. Crystallogr.*, **1935**, *58*, 6.

(13) Lind, M.D.; *Acta Crystallogr. B.*, **1970**, *26*, 1058.

(14) Grant, R.W.; *J. App. Phys.*, **1971**, *42*, 1619. Grant, R.W.; Wiedersich, H.; Housley, R.M.; Espinosa G.P.; Artman, J.O. *Phys. Rev. B*, **1971**, *3*, 678.

(15) Gol'danskii Vitalii I.; Makarov, E.F. in "Chemical Applications of Mössbauer Spectroscopy" Gol'danskii, V.I. Herber, R.H., Eds.; Academic Press: New York 1968. Flinn, Paul; Ruby, S.L.; Kehl, W.L. *Science (Washington D.C.)*, **1964**, *143*, 1434; Herber, R.H.; Chanda, S. *J. Chem. Phys.*, **1971**, *54*, 1847.

(16) Meyer, S.F.; Howard, R.E.; Stewart, G.R.; Acrivos, J.V.; Geballe, T.H. *J. Chem. Phys.*, **1975**, *62*, 4411. DiSalvo, F.J.; Bagley, B.G.; Voorhoeve, J.M.; Waszczak, J.V. *J. Phys. Chem. Solids*, **1973**, *34*, 1357.

intercalates of this matrix[19] with compositions of $TaS_2 \cdot Sn_{1/3}$ and $TaS_2 \cdot Sn$, with T_c's of <0.5 and 3.2 K, respectively. A ^{119}Sn Mössbauer study by DiSalvo et al.[17] had shown that the resonance spectrum of $TaS_2 \cdot Sn_{1/3}$ consists of a singlet peak at an isomer shift of 3.85 ± 0.02 mm s^{-1} at 78 K. In contrast, the resonance spectrum of $TaS_2 \cdot Sn$ shows two resonance maxima with an energy difference of 1.15 ± 0.01 mm s^{-1}.

Clearly, the latter spectrum can be interpreted in two plausible ways: (a) there are two approximately equally populated tin sites in the layer compound structure, each giving rise to a singlet resonance line; or (b) there is a unique tin site giving rise to a quadrupole split doublet. The observation that one of the two resonance maxima observed in the $TaS_2 \cdot Sn$ spectrum (2.53 mm s^{-1} with respect to $BaSnO_3$) lies very close to that of β-Sn (2.55 mm s^{-1}), while the second maximum (3.77 mm s^{-1}) lies very close to that observed for the tin atom in $TaS_2 \cdot Sn_{1/3}$ (3.84 mm s^{-1}), gave rise to the speculation that there are, in fact, two tin sites in $TaS_2 \cdot Sn$ corresponding to metallic tin and the $TaS_2 \cdot Sn_{1/3}$ type of site, respectively. This speculation is also supported by an electron configuration interpretation, in which the d_{z^2} band of tantalum in 2H-TaS_2 can accommodate only a single additional electron, and thus the oxidation $Sn \rightarrow Sn^{2+} + 2e^-$ can only involve up to one-half of the tin atoms in a material having a Ta:Sn ratio of 1:1. Thus, on this basis, half the tin atoms are formally 2+ and half have the electron configuration of metallic tin, giving rise to two distinct tin atoms within the structure of $TaS_2 \cdot Sn$.

On the other hand, powder pattern X-ray data over the whole compositional range $0.2 < n < 1.0$ for $TaS_2 \cdot Sn_n$ showed that in the interval $0.33 < n < 1.0$, only mixed phases (presumably $TaS_2 \cdot Sn_{1/3}$ and $TaS_2 \cdot Sn$) were present. This observation suggests that not more than one-third of the tin atoms in $TaS_2 \cdot Sn$ could be present in the type of site found in $TaS_2 \cdot Sn_{1/3}$. This observation is inconsistent with the analysis of the Mössbauer data on the basis of two essentially equally populated distinct tin sites and could be understood only on the basis of a single site in $TaS_2 \cdot Sn$. The choice between these two alternatives appeared to have been decided by a subsequent study[19] of the wide-band NMR spectra of $TaS_2 \cdot Sn$ that showed only a single wide asymmetric resonance line with $K_{\parallel} = +(0.69 \pm 0.02)\%$ and $K_{\perp} = +(0.81 \pm 0.02)\%$. On the basis of this observation, it was concluded that the ^{119}Sn Mössbauer spectrum could be understood as arising from a single tin site giving rise to a quadrupole split resonance pattern.

Subsequently, however, the ESCA spectrum of $TaS_2 \cdot Sn$ has been studied,[20] and the $3d_{3/2}$ and $3d_{5/2}$ electron region was observed to consist of two distinct maxima for each type of electron. Since the NMR data[19] could be accounted for either by a fortuitous superposition of two ^{119}Sn resonances (i.e., identical Knight shifts of two distinct tin sites) or by the anomalous (relaxation) broadening of one of the ^{119}Sn NMR

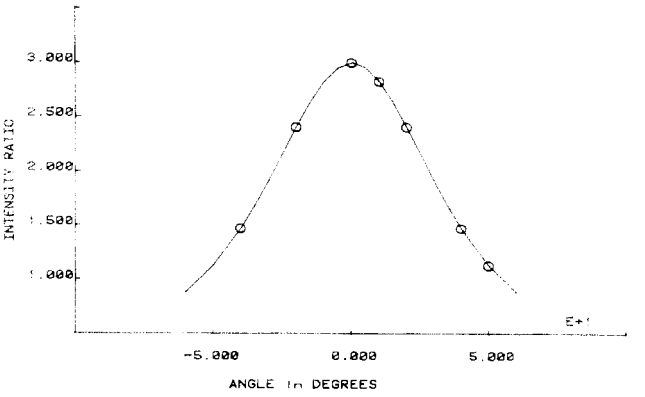

Figure 2. Angular dependence of the area ratio of the doublet in $TaS_2 \cdot Sn$ for the ^{119}Sn resonance. The solid line is that calculated from the theoretical angular dependence of $I(\pi)/I(\sigma)$ (ref 22); the circles are the observed experimental points corrected for geometric errors. The abscissa extends from −60 to +60°.

resonance signals, the photoelectron spectroscopic data again raised an uncertainty concerning the question of whether the ^{119}Sn Mössbauer spectrum arises from one tin site or two.

The resolution of this problem was effected by carrying out a single crystal study[21,22] of 2H-$TaS_2 \cdot Sn$ in which the relative intensity of the two resonance maxima is studied as a function of the angle between the crystallographic symmetry axis and the optical (γ-ray beam) axis of the Mössbauer experiment. The results of this experiment are summarized graphically in Figure 2 and show unambiguously that the doublet resonance spectrum arises from a single tin site in the intercalation compound. This site has a nonvanishing electric field gradient and thus accounts for the presence of the quadrupole split doublet. The interpretation of the ESCA results, which at first glance seem to be at variance with the ^{119}Sn Mössbauer data, has been suggested by Wertheim,[20] who pointed out that in an ESCA experiment on a freshly cleaved sample of $TaS_2 \cdot Sn$, one normally probes only the first few layers below the surface, while in a Mössbauer experiment one "sees" the bulk solid. Thus, the ESCA results of Eppinga et al.,[23] which seemed to suggest the presence of two different kinds of tin atoms in $TaS_2 \cdot Sn$, can be understood in terms of the presence of a partial layer of Sn atoms on the (cleaved) surface and the Sn atoms in the next layer(s). The two kinds of tin atoms clearly will have different electron energetics and hence give rise to different ESCA spectra.

The unusual linear S–Sn–S array in $TaS_2 \cdot Sn$[24] and the observed isomer shift of 3.2 mm s^{-1} at 78 K which indicated that the tin was present in an oxidation state that could formally be characterized as "stannous" prompted an additional Mössbauer investigation[25] of this intercalate. This study was motivated by the question whether the transfer of a single electron from Sn to Ta (which requires only one electron to fill the d_{z^2} band in tantalum) leaves enough unpaired spin density on the tin to give rise to an appreciable magnetic hyperfine field on Sn at low temperatures. ^{119}Sn Mössbauer effect studies[25] at 4.2 K in the presence of

(17) DiSalvo, Frank J.; Hull, G.W. Jr.; Schwartz, L.H.; Voorhoeve, J.M.; Waszczak, J.V. *J. Chem. Phys.*, **1973**, *59*, 1922.
(18) Gamble, Fred R.; DiSalvo, F.J.; Klemm, R.A.; Geballe, T.H. *Science (Washington D.C.)*, **1970**, *168*, 569.
(19) Gossard, A.C.; DiSalvo, F.J.; Yasuoka, H. *Phys. Rev. B*, **1974**, *9*, 3965.
(20) Haas, C. private communication. Wertheim, G.K. private communication.
(21) Herber, Rolfe H.; Davis, R.F. *J. Chem. Phys.*, **1975**, *63*, 3668.
(22) Herber, Rolfe H.; Davis, R.F. *J. Chem. Phys.*, **1976**, *65*, 3773.
(23) Eppinga, R.; Sawatzky, G.A.; Haas, C.; van Bruggen, C.F. *J. Phys. C*, **1976**, *9*, 3371.
(24) Eppinga, R.; Wiegers, G.A. *Mater. Res. Bull.*, **1977**, *12*, 1057.

Table I
Summary of Mössbauer Data for NbS_2 and TaS_2 Intercalation Compounds with Tin

absorber	IS(78 K), mm s^{-1}	dIS/dT, mm s^{-1} deg^{-1}	QS(78 K), mm s^{-1}	$-\mathrm{d} \ln \frac{A(T)}{A(78)} / \mathrm{d}T$, deg^{-1}	θ_M, deg	ref
$TaS_2 \cdot Sn_{1/3}$	3.851	-4.44×10^{-4}		3.48×10^{-4}	233 ± 10	21, 22
$NbS_2 \cdot Sn_{1/3}$	3.681	-2.17×10^{-4}		4.61×10^{-3}	197 ± 5	28
$TaS_2 \cdot Sn$[a]	3.13	-3.38×10^{-4}	1.09		176 ± 5	21, 22
$TaS_2 \cdot Sn$	3.192		1.15	5.50×10^{-3}	185 ± 10	21, 22
$NbS_2 \cdot Sn$	3.134	-3.4×10^{-4}	0.954	7.03×10^{-3}	159 ± 5	28

[a] Single crystal sample.

Table II
Summary of Mössbauer Data for Anhydrous $FeCl_3$, and $FeCl_2$ and $FeCl_3$ Graphite Intercalation Compounds[a]

compound	isomer shift,[b] mm s^{-1} 78 K	300 K	$-$dIS/dT, mm s^{-1} deg^{-1}	quadrupole splitting, mm s^{-1} 78 K	300 K	$-\mathrm{d} \ln \frac{A(T)}{A(78)} / \mathrm{d}T$, deg^{-1}	θ_M, deg
graphite-$FeCl_3$	0.53	0.49	5.18×10^{-4}			5.08×10^{-3}	164 ± 5
graphite-$FeCl_2$							
Fe(b)	1.23	1.09	6.56×10^{-4}	1.11	0.79	5.17×10^{-3}	162 ± 5
Fe(a)	1.23	1.09	6.68×10^{-4}	1.96	1.60	4.67×10^{-3}	171 ± 5
$FeCl_3$	0.55	0.43	7.28×10^{-4}			2.68×10^{-3}	225 ± 5

[a] The lattice temperatures (θ_M) are calculated by using the atomic mass for the Mössbauer-active atom. All data from ref 44 and 45. [b] With respect to the center of a 295-K α-Fe spectrum obtained, with the same ^{57}Co source.

external magnetic fields of 0, 50, and 80 kOe confirmed the fact that there is, in fact, no significant unpaired electron density localized on the tin atom and that the isomer shift which is observed is appropriate to a stannous moiety held in the structure by what are predominantly covalent chemical bonding forces. The total coordination of tin—including six nearest-neighbor metal atoms in the van der Waals layer—is eight, and it is reasonable to assign the p_z and d_{z^2} orbitals of the tin to the bonding interaction in the linear S–Sn–S array that is present in $TaS_2 \cdot Sn$.[26]

A closely related intercalation system is that based on niobium sulfide, which—like its tantalum homologues—gives rise to two well-defined compounds, $NbS_2 \cdot Sn_{1/3}$ and $NbS_2 \cdot Sn$. Eppinga and Wiegers[27] had shown that the niobium compounds are isostructural with the tantalum intercalates, thus affording a direct comparison of the lattice dynamical properties of the two systems. As expected from the crystallographic data, the ^{119}Sn Mössbauer spectra of $NbS_2 \cdot Sn_{1/3}$ and $NbS_2 \cdot Sn$ consist[28] of a singlet and doublet resonance pattern, respectively, and the earlier interpretation of the TaS_2 data[21,22] is directly applicable to the NbS_2 system. A comparison of these data is summarized in Table I. From this table it is noted that the lattice temperature, θ_M, calculated from the temperature dependence of the recoil-free fraction, is significantly lower in the case of the niobium sulfide intercalates than in the corresponding tantalum compounds. These lattice temperature differences probably arise from the greater covalency of the metal sulfur bond in the former as compared to the latter, as well as the differences in the Sn–Nb and Sn–Ta interactions themselves. These differences are also reflected in a comparison of the quadrupole hyperfine interaction in the two compounds. This interaction (at 78 K) is ~15% smaller in $NbS_2 \cdot Sn_{1/3}$ than in the corresponding tantalum compound. In both compounds the relative intensity of the two components of the quadrupole split spectrum is temperature dependent and thus presumably originates in an anisotropy of the vibrational amplitude of the Mössbauer active atom parallel and perpendicular to the local symmetry axis through the Sn atom. This difference in the mean square vibrational amplitudes in $TaS_2 \cdot Sn_{1/3}$ at 295 K is 4.65×10^{-18} cm^2, whereas the corresponding value in $NbS_2 \cdot Sn_{1/3}$ is 1.3×10^{-18} cm^2 at 300 K.

Fe. A large number of investigations exploiting the 14.4-keV Mössbauer transition in ^{57}Fe have been reported,[6,29,30] including detailed studies of $NbS_2 \cdot Fe_{1/3}$ and the related titanium homologues $TiS_2 \cdot Fe_x$ ($x = {}^1/_4$, ${}^1/_3$, and ${}^1/_2$).[31,32,33] Among the most detailed Mössbauer studies of intercalation compounds are those involving atomic and molecular guest species in graphite, which use matrices of randomly oriented microcrystals, highly oriented pyrolytic graphite (HOPG), or exfoliated two dimensionally ordered material (GRAFOIL).[34] The lamellar compounds C_8Cs and $C_{24}Cs$ were studied by Campbell, Montet, and Perlow,[35] who made use of the

(25) Herber, Rolfe H.; DiSalvo, F.J.; Frankel, R.B. *Inorg. Chem.*, **1980**, *19*, 3135.
(26) See footnote 16 in ref 25.
(27) Eppinga, R.; Wiegers, G.A. *Physica B + C (Amsterdam)* **1980**, *99*, 121.
(28) Herber, Rolfe H.; Katada, M. *J. Solid State Chem.*, **1979**, *27*, 137.
(29) Eibschutz, Marcu; Disalvo, F.J. *Phys. Rev. Latt.*, **1976**, *36*, 104. Eibschutz, M.; Lines, M.E. *Phys. Rev. Lett.*, **1977**, *39*, 726.
(30) Halbert, Thomas R.; Scanlon, J.C. *Mater. Res. Bull.*, **1976**, *14*, 415. Revelli, J.F.; Ratajack, M.T.; Gleizes, A.; Schwatz, L.; Wagner, J.B.; Kannewurf, C.R. *Bull. Amer. Phys. Soc.*, **1975**, *20*, 487.
(31) Katada, Motomi; Herber, R.H. *J. Solid State Chem.*, **1980**, *33*, 361.
(32) Fatseas, G.A. Dormann, J.L. Danot, M. *J. Phys.*, **1976**, *37C6*, 579; **1979**, *40C2*, 367. van den Berg, J.M.; Cossee, P. *Inorg. Chim. Acta*, **1968**, *2*, 143.
(33) Takahashi, T.; Yamada, O. *J. Solid State Chem.*, **1973**, *7*, 25.
(34) Hennig, G.R. *Prog. Inorg. Chem.*, **1959**, *1*, 125. Rudorff, W. *Adv. Inorg. Chem. Radiochem.*, **1959**, *1*, 233. Ubbelohde, A.R.; Lewis, F.A. "Graphite and its Crystal Compounds"; Oxford Press: Oxford, 1960. Fischer, J.E. *Physica B* **1980**, *99*, 383. Ebert, L.B. *Annu. Rev. Mater. Sci.*, **1976**, *6*, 181. Fischer, J.E.; Thompson, T.E. *Phys. Today*, **1978**, July, p 36. Gamble, F.R.; Geballe, T.H. in "Treatise on Solid State Chemistry", Hannay, N.B. *Ed.*, Plenum Press: New York, 1975.
(35) Campbell, L.E.; Montet, G.L.; Perlow, G.J. *Phys. Rev. B*, **1977**, *B15*, 3318.

81-keV Mössbauer transition in ^{133}Cs to determine the anisotropy of the recoil-free fraction at 4.2 K. Their isomer shift data indicate that the alkali metal is fully ionized in $C_{24}Cs$ and about 50% ionized in C_8Cs. Ballard and Birchall[36] have used the 37.2-keV transition in ^{121}Sb to study the Mössbauer effect of SbF_5 and $SbCl_5$ intercalated into graphite.[37] On intercalation into the graphite layers, a portion of the pentavalent antimony is reduced to the trivalent state, and resonance absorptions characteristic of both oxidation states are observed in the spectra at liquid helium temperature.

Several detailed studies of iron halides intercalated into graphite have been reported,[38-43] including the systems $FeCl_3$–graphite[41] and $FeCl_3/AlCl_3$–graphite,[43] and the charge states of the guest species under various conditions have been inferred from the spectroscopic data. Most of the Mössbauer investigations have focused on the isomer shift parameter, without addressing the lattice dynamical properties of the anisotropy host matrix as probed by the guest species.

Such experiments have been carried out[44,45] on both $FeCl_3$ and $FeCl_2$ intercalated graphite, the latter having been prepared by reducing the first stage ferric chloride intercalate ($C_{10}FeCl_3$) in flowing hydrogen at 375 °C. In the graphite–$FeCl_3$ intercalation compound, the temperature dependence of the isomer shift of the singlet resonance peak has a significant contribution from the electron donation of the lattice to the d orbital(s) of the metal atom. The ^{57}Fe Mössbauer data are summarized in Table II. The lattice temperature calculated from the recoil-free fraction data for the intercalate yields a value of 164 ± 5 K compared to a value of 225 ± 5 K for anhydrous $FeCl_3$. These data suggest that the iron moiety packing in the intercalation compound is looser than that in anhydrous $FeCl_3$ and that the metal atom in the former is more mobile than in the latter and executes a larger vibrational motion at a given temperature in the layer structure.

In contrast to the results for the $FeCl_3$ intercalate, the Mössbauer spectra of the reduced species in the graphite matrix show[44] the presence of two distinct iron species, referred to as Fe(a) and Fe(b). These two iron resonances have not only essentially the same isomer shift (1.23 mm s^{-1} at 78 K with respect to metallic iron at 295 K), but also this isomer shift is similar to that of anhydrous (neat) $FeCl_2$, indicating the absence of significant electron transfer from the π system of the lattice to the metal atoms. The quadrupole splitting of the two sites is, however, quite different. The value for Fe(b) is about the same as for anhydrous $FeCl_2$ (1.11 mm s^{-1} at 78 K), while that of Fe(a) is about 1.96 mm s^{-1}. For both iron sites in the graphite matrix, the lattice temperature is about the same [162 ± 5 and 171 ± 5 K, respectively, for Fe(a) and Fe(b)]. However, a single crystal orientation experiment shows that the anisotropy of motion is much larger for Fe(b) than for Fe(a). This conclusion is based on the observation that the intensity ratio, R, for the $\pi(\pm^1/_2 \rightarrow \pm^3/_2)$ and $\sigma(\pm^1/_2 \rightarrow \pm^1/_2)$ transitions is strongly dependent on the angle θ between the normal to the easy cleavage plane of the graphite single crystal and the optical (γ ray) axis of the experiment.

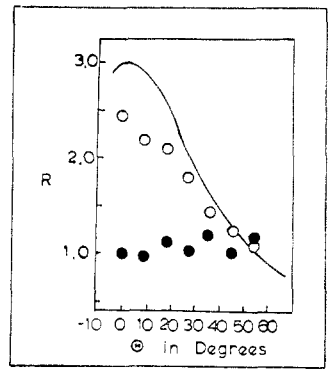

Figure 3. Intensity ratio $R = I(\pi)/I(\sigma)$ for the Fe(a) (●) and Fe(b) (○) sites in a single crystal sample of the $FeCl_2$-graphite intercalation compound at 295 ± 2 K. The angle θ refers to the orientation of the optical (γ-ray propagation) axis with respct to the crystallographic c axis.

The results of such an experiment are summarized graphically in Figure 3, from which it is seen that the intensity ratio of the π to the σ transition for Fe(a) is essentially independent of θ while this ratio is strongly angle dependent for the Fe(b) site. These results imply that the bonding of the iron atoms that give rise to the Fe(b) resonance is strongly anisotropic while the bonding of the iron atoms in the Fe(a) site does not share in the anisotropy of the graphite lattice. Further Mössbauer effect studies of this motional anisotropy, and its relationship to the structural anisotropy of the graphite host lattice, represent a fruitful area of study. Unfortunately, the range of iron compounds that can be intercalated into graphite without disruption of the host lattice is severely limited, and new synthetic approaches are required to permit exploitation of the full possibilities of the Mössbauer technique in the elucidation of motional anisotropy in these intercalates.

Study of Host Matrices

In the preceding discussion, it was seen that the requirement that the guest species contain a Mössbauer-active atom placed a severe constraint on the range of materials available for study by this technique. By contrast, if the host matrix itself contains a suitable atom for Mössbauer studies, an extended range of systems can be examined, permitting subtle and systematic changes in size, stereochemistry, and chemical behavior of the guest species. It should be borne in mind, however, that in these cases the probe atom is part of the continuum into which the guest species is placed. Hence, the probe may be relatively far removed from the actual site of the guest–host interaction and the observed effects may be of a second-order nature rather than reflecting directly the interaction under study.

(36) Ballard, Jack G.; Birchall, T. *J. Chem. Soc., Dalton Trans.*, **1976**, 1859.
(37) Lalancette, J.M.; Lafontaine, J. *J. Chem. Soc., Chem. Commun.*, **1973**, 815.
(38) Mele, E.J.; Ritsko, J.J. *Phys. Rev. Lett.* **1979**, *43*, 68.
(39) Ohhashi, K.; Tsukikawa, I. *J. Phys. Soc. Jpn.*, **1974**, *36*, 422. Hooley, J.G.; Bartlett, M.W.; Liengme, B.V.; Sams, J.R. *Carbon*, **1968**, *6*, 681.
(40) Wertheim, Gunther K.; van Attekum, P.M.Th.M.; Guggenheim, H.J.; Clements, K.E. *Solid State Commun.*, **1980**, *33*, 809.
(41) Saito, N.; Tominaga, T.; Takeda, M.; Ohe, Y.; Ambe F.; Sano, H. *Nippon Arsatapu Kaigi Hobunshu*, **1967**, 231.
(42) Freeman, A.G. *J. Chem. Soc., Chem. Commun.*, **1968**, 193.
(43) Tominaga, Takeshi; Sakai T.; Kimura, T. *Bull. Chem. Soc. Jpn.*; **1976**, *49*, 2755.
(44) Katada, Motomi; Herber, R.H. *J. Phys. Collog. (Orsay, Fr.)* **1979**, *40C2*, 663.
(45) Herber, R.H.; Katada, M. *J. Inorg. Nucl. Chem.*, **1979**, *41*, 1097.

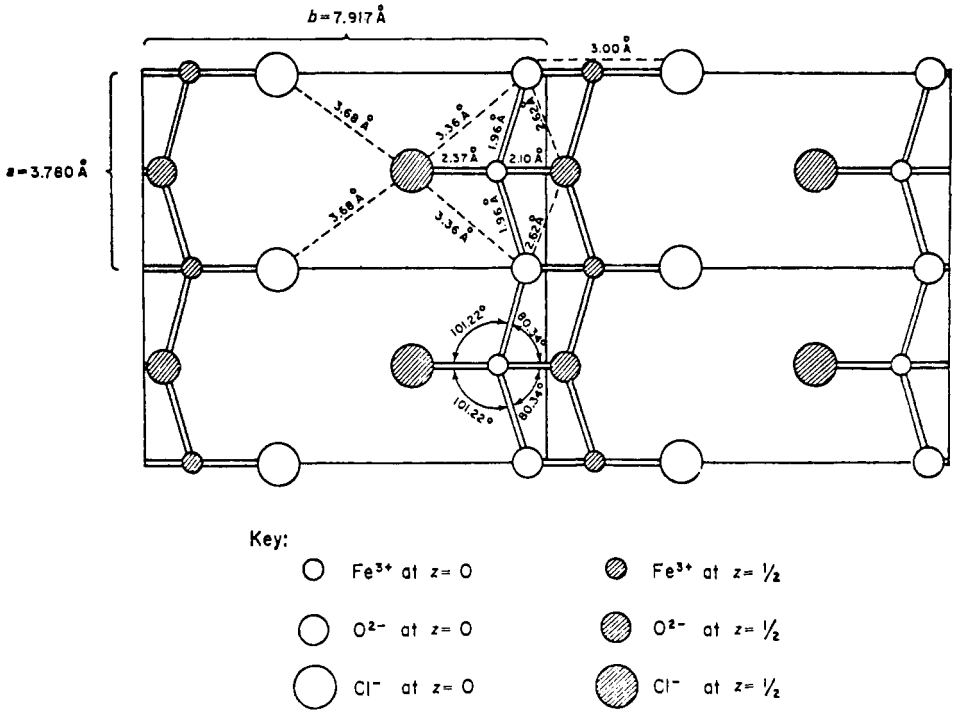

Figure 4. Structure of FeOCl on (001) showing four complete unit cells. (Reprinted with permission from ref 13. Copyright 1970 by the International Union of Crystallography.)

Table III
Summary of Mössbauer and X-ray Data for Some of the FeOCl Intercalates Discussed in the Text

intercalant	IS, 78 K, mm s^{-1}	QS, 78 K, mm s^{-1}	n^a	b, Å	θ_M,[b] deg	H_i,[e] kOe	ref
-	0.511 ± 0.008[c]	0.929 ± 0.010[c]		7.91	341 ± 4	432 ± 1	50, 47
pyridine	0.477 ± 0.030	1.252 ± 0.022	1/3	13.45	200 ± 6	441 ± 1	50
α-picoline	0.517 ± 0.010	1.197 ± 0.024	1/3		242 ± 7		
α-picoline *N*-oxide	0.503 ± 0.017	1.146 ± 0.015	1/4	13.52	247 ± 8[d]	443 ± 1	
pyridine *N*-oxide	0.504 ± 0.010	1.169 ± 0.023	1/3		220 ± 7		50
TED[f]	0.509 ± 0.010	1.010 ± 0.008	1/6	13.06	243 ± 8		51
Kryptofix-22	0.509 ± 0.010	1.128 ± 0.010	1/18	12.2	197 ± 8	434 ± 1	53
Diaz	0.508 ± 0.010	1.210 ± 0.010	1/3	13.33	219 ± 8	439 ± 1	
$(CH_3O)_3P$	0.506 ± 0.036	1.153 ± 0.009	1/6	14.38	219 ± 1	431 ± 1	52
$(C_2H_5)_3P$	0.447 ± 0.074	1.194 ± 0.025	1/6	11.87	203 ± 2	435 ± 1	52

[a] n is the stoichiometry descriptor in $FeOCl(G)_n$. [b] Mössbauer lattice temperature calculated by using the atomic mass for the Mössbauer active atom. [c] Extrapolated from data above the magnetic ordering temperature. [d] For the temperature range $100 \leq T \leq 225$ K. [e] The magnetic field at the Fe nucleus at 4.2 K. [f] Triethylenediamine.

One of the most interesting intercalation matrices which contains a Mössbauer active atom is iron oxychloride, FeOCl, which is capable of accommodating a wide variety of guest species. These include single electron donors such as Li and ferrocene, which reside in the matrix in the cationic form, and electron pair donors such as NH_3, pyridine, and related compounds, which are presumably present as neutral entities. FeOCl itself consists of double rows of cis-octahedral iron centers so arranged that the halogen atoms form the outermost layers. These chlorine layers face each other and constitute the van der Waals easy-cleavage plane into which guest molecules can be inserted. The crystal structure of FeOCl has been studied in great detail,[12,13] and a two-dimensional representation of the atom arrangement is shown in Figure 4.

The Mössbauer parameters of FeOCl have also been reported in detail, and the pertinent data are included in Table III. The isomer shift and quadrupole parameters are characteristic of high-spin Fe(III). The magnetic hyperfine field at the iron atom at 4.2 K is[46,47] 432.2 ± 1.0 kOe, considerably lower than the value of 550 kOe expected for a d^5 high spin ferric ion. This reduction in the internal magnetic field arises from covalency effects in the bonding of the metal atom to its nearest-neighbor environment. The ^{57}Fe Mössbauer spectrum of FeOCl at 4.2 K is shown in Figure 5.

As expected from the cis-octahedral arrangement of the atoms bonded to the metal atom, the ^{57}Fe Mössbauer spectrum shows the expected quadrupole split doublet. Of particular interest with respect to the study of FeOCl intercalates is the observation that the temperature dependence of the QS parameter in pure FeOCl is exceptionally small.[14] The difference between the room temperature and liquid nitrogen temperature values amounts to only 1.2×10^{-3} mm s^{-1} or an average change of $\sim 6 \times 10^{-6}$ mm s^{-1} K^{-1} over this range.

Finally, with respect to the characteristics of the unintercalated matrix, it is interesting to note that magnetic ordering effects start to be noted in the Mössbauer spectra on cooling to ~90 K. However, in

(46) Kostiner, E.; Steger, J. *J. Solid State Chem.*, **1971**, *3*, 273.

(47) Herber, Rolfe H.; Maeda, Y. *Physica B + C (Amsterdam)*, **1980**, *99B*, 352.

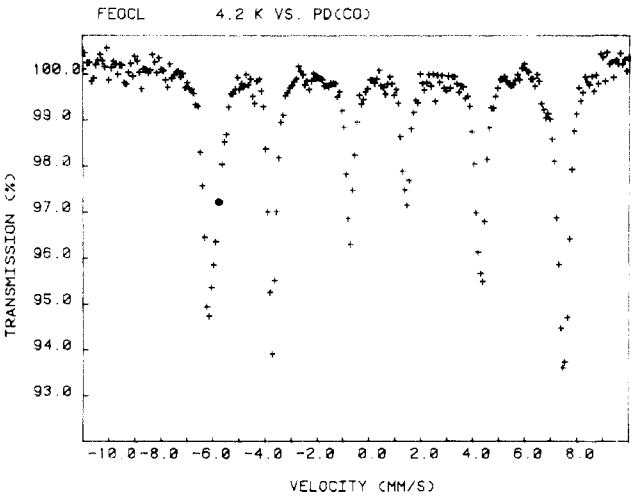

Figure 5. Mössbauer effect spectrum of FeOCl at liquid helium temperature. The sign of V_{zz} can be calculated from the relative separation of the two outermost peaks on each side of the center. The internal magnetic hyperfine field at the ^{57}Fe nucleus can be calculated from the positions of the two outermost peaks.

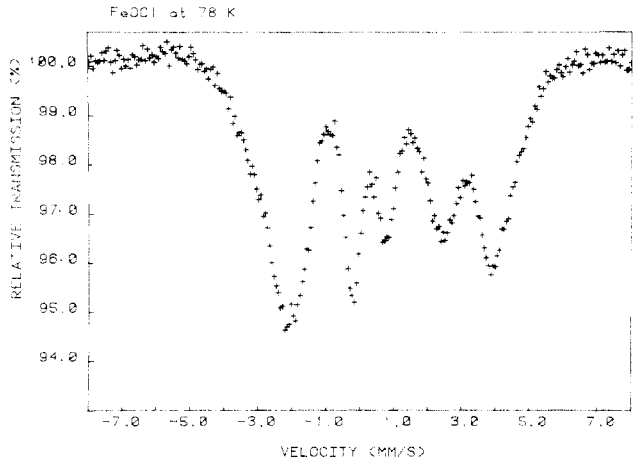

Figure 6. Mössbauer effect spectrum of FeOCl at liquid nitrogen temperature. The broad resonance lines and the relative intensities of the components are characteristic of magnetic relaxation phenomena in this solid, in contrast to the sharp onset of magnetic ordering in metallic iron at 1046 K.

contrast to materials showing a sharp first-order phase transition from a paramagnetic to a ferromagnetic (or antiferromagnetic) state at the magnetic ordering temperature, the Mössbauer spectra of FeOCl show a gradual change from the two-line spectrum characteristic of the paramagnetic state to a spectrum characteristic of the magnetically ordered state as the sample is cooled. The Mössbauer spectrum of unintercalated FeOCl at liquid nitrogen temperature (~78 K) is shown in Figure 6.

Our recent work in this field has focussed on FeOCl intercalates in which the guest species are Lewis base electron pair donors. Typical of such systems is FeOCl–pyridine which has been extensively studied by a number of research groups, especially that of Kanamaru in Japan.[48]

On soaking FeOCl in liquid pyridine, several well-defined intercalation compounds can be produced.

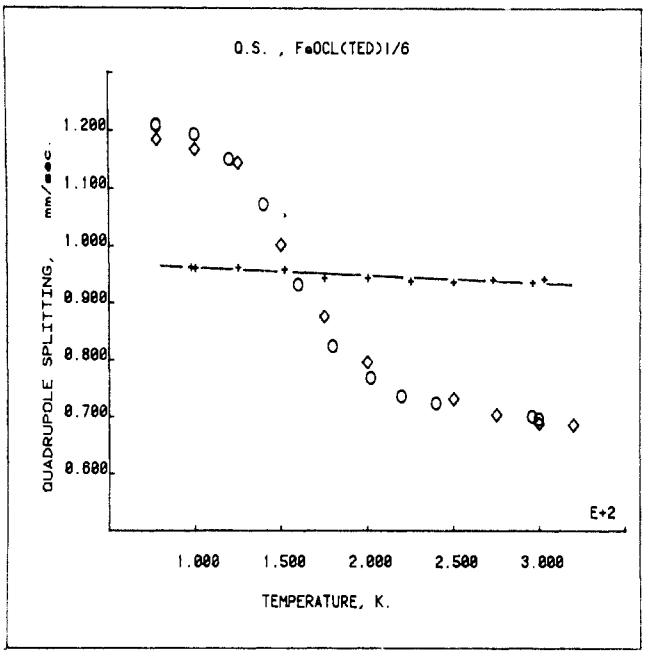

Figure 7. Termperature dependence of the quadrupole splitting parameter is $FeOCl(TED)_{1/6}$. The comparable data for unintercalated FeOCl is shown by the crosses. The circles and diamonds represent two replicate samples and indicate the reproducibility of the data.

While the particular stoichiometry which is achieved depends on the temperature and length of time of the intercalation process, the systems $FeOCl(py)_{1/3}$, $FeOCl(py)_{1/4}$, and $FeOCl(py)_{3/4}$ have been reported.[48,49] Intercalations of the Lewis base result in a dramatic increase in the crystallographic *b* parameter, while the *a* and *c* parameters of the unit cell are essentially unaffected. The *b* parameter in FeOCl itself is 7.917 ± 0.005 Å. In $FeOCl{\cdot}py_{1/3}$ this parameter increases by almost 6 Å, and corresponding *b* parameter increases have been determined for substituted pyridines and alkylamines.[49] In the case of pyridine, the molecular dimensions in the ring plane either parallel or perpendicular to the twofold symmetry axis are nearly the same, so that the *b*-axis expansion which is observed does not answer the question of the orientation of the guest molecule with respect to the host, except that the orientation in which the ring plane is oriented parallel to the FeOCl *b* axis can be excluded. Data relating to the observed *b*-axis expansion are summarized in Table III.

An especially interesting intercalation system is that formed between FeOCl and triethylenediamine (diazabicyclo[2.2.2]octane), $FeOCl(TED)_{1/6}$, and this material has been studied in detail by ^{57}Fe Mössbauer effect spectroscopy.[50] Of particular interest is the temperature dependence of the quadrupole hyperfine interaction.[51] As already noted above, this parameter varies only slightly with temperature in unintercalated FeOCl. On the other hand, in $FeOCl(TED)_{1/6}$ the QS parameter undergoes a very large change in the temperature range $78 \leq T \leq 320$ K, as shown graphically in Figure 7. From this figure—in which the QS for FeOCl is shown in comparison to the value in the intercalate—it is seen

(48) Kanamaru, F.; Koizumi, M. *Jpn. J. App. Phys.*, **1974**, *13*, 1319. Kanamaru, F.; Yamanaki, S.; Koizumi, M.; Nagai, S. *Chem. Lett.*, **1974**, 373. Kanamaru, F.; Shimada, M.; Koizumi, M.; Takano, M.; Takada, T. *J. Solid State Chem.*, **1973**, *7*, 297.

(49) Hagenmuller, P.; Portier, J.; Barbe B.; Bouclier, P. *Z. Anorg. Allg. Chem.*, **1967**, 355, 209. Kanamaru, F.; Yamanaka S.; Koizumi, M. *Bull. Chem. Soc. Jpn.*, **1979**, *52*, 963.

(50) Herber, Rolfe H.; Maeda, Y. *Inorg. Chem.*, **1981**, *20*, 1409.

(51) Herber, Rolfe H.; Rein, A. J. *J. Chem. Phys.*, **1980**, *73*, 6345.

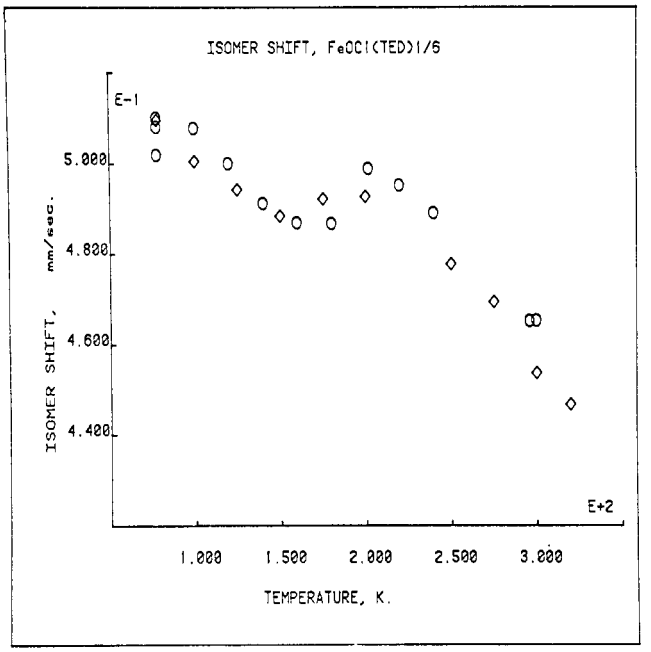

Figure 8. Temperature dependence of the isomer shift parameter in $FeOCl(TED)_{1/6}$. The low temperature regime and the high temperature regime have significantly different slopes, reflecting the tighter binding of adjacent layers of the solid below ~150 K as compared to the temperature range (above ~220 K) where the interlayer vibrations become soft with respect to thermal excitation of the lattice.

that at low temperatures the QS is considerably larger than it is in the neat matrix, and falls to a considerably smaller value at high temperatures. Moreover, the limiting slope at high temperatures approaches that of unintercalated FeOCl.

These observations can be understood in terms of a model that envisions a transition in the intercalate from a three-dimensional solid at low temperatures to a quasi-two-dimensional solid at high temperatures. Near liquid nitrogen temperature, the binding forces across the van der Waals layer are large compared to the mean thermal excitation of the lattice, and normal thermal expansion accounts for the temperature dependence of QS. As the thermal excitation energy is raised on warming, this energy becomes larger than the interlayer bonding energy, and ultimately the two adjacent FeOCl double layers can exhibit a relatively soft motion parallel to the easy cleavage plane. The quadrupole interaction is largely a reflection of the bond angles (and distances) about the iron atom. In the quasi-two-dimensional solid regime (i.e., above ~150 K) the Cl–Fe–Cl bond angle has relaxed to a value giving a significantly smaller QS in the intercalate in which the interlayer distance is large, as compared to the unintercalated lattice in which the interlayer distance is governed by the chlorine–chlorine contacts. The temperature dependence of $QS(T)$, that is, $d(\Delta QS/\Delta T)/dT$ shows a maximum at ~153 K with a full width at half-maximum of about 60°, indicative of a relatively slow transition from the low temperature to the high temperature form.

The isomer shift parameter, which also reflects the details of the electronic environment around the iron atom, shows a temperature dependence which is consistent with the above model, and is summarized for $FeOCl(TED)_{1/6}$ in Figure 8. The temperature dependence of the isomer shift is related to the motion of the iron atom and hence to the bonding of the iron atom to its environment. The change in slope of $IS(T)$ at ~150 K is once again an indication of the transitions from the low temperature to the high temperature structure in the FeOCl intercalate.

Finally, in the context of this discussion, it should be noted that the interlayer interaction referred to above, which dominates the temperature dependence of the QS parameter, results in a vibrational mode which is infrared active. A search of the lattice mode (far-infrared) region of the spectrum of unintercalated and intercalated FeOCl has shown that a band which is observed at 184.4 cm^{-1} in FeOCl is red-shifted to 165.2 cm^{-1} in $FeOCl(TED)_{1/6}$ at room temperature. This latter frequency corresponds reasonably well with the peak in the $d(\Delta QS/\Delta T)/dT$ curve at ~153 K and has been tentatively identified[51] with the interlayer vibration across the van der Waals gap in the solid.

In addition to the pyridine related intercalants discussed above, a number of other chemically interesting guest molecules can be introduced into the FeOCl matrix. Typical of such species are $(CH_3O)_3P$ and $(C_2H_5)_3P$, both of which give rise to intercalates with a guest to host ratio of 1:6 and for which detailed ^{57}Fe Mössbauer effect data have been published.[52] Among the largest Lewis base guest molecules that have so far been successfully intercalated into FeOCl are the two polyethers, 1,7,10-trioxa-4,13-diazacyclopentadecane (Kryptofix-21) and 1,7,10,16-tetraoxa-4,13-diazacyclooctadecane (Kryptofix-22). The two systems that have been studied[53,54] both have the stoichiometry $FeOCl(guest)_{1/18}$ (which appears to be the limiting stoichiometry obtained at 73 °C in ethanol after 4 weeks), and there is some evidence that both nitrogen atoms of the polyether are involved in bonding to the metal atoms of the host lattice. The detailed study of the chemical bonding forces that hold such molecules in the van der Waals layers of the matrix and the modifications in the chemical and physical properties of both the guest and the host moieties that occur on intercalation provide a fruitful field of further study for both the experimentalist and the theoretician interested in these anisotropic materials.

Concluding Remarks

The detailed study of molecular intercalation compounds by Mössbauer effect spectroscopy has already revealed a wealth of information about such systems. Much of this information would be difficult to obtain by the use of other techniques. However, a great deal of further systematic study of guest–host interactions in these types of compounds holds the promise of providing deeper insights into the dynamical and chemical properties of intercalates. Particularly interesting is the study of organometallic guest species in the host lattice. Halbert and Scanlon[55] and Halbert et al.[6] have reported the preparation of cobalticene and ferrocene intercalates of FeOCl, and similar compounds have been prepared by Schäfer-Stahl and co-workers[56] and studied by X-ray diffraction, differential thermal analysis,[57] and

(52) Herber, Rolfe H.; Maeda, Y. *Inorg. Chem.* **1980**, *19*, 3411; *Physica B + C (Amsterdam)*, **1981**, *105B*, 243.
(53) Herber, Rolfe H.; Cassell, R. *J. Chem. Phys.*, **1981**, *75*, 4669.
(54) Herber, Rolfe H.; Cassell, R. *Inorg. Chem.*, in press.
(55) Halbert, Thomas T.; Scanlon, J. *Mater. Res. Bull.*, **1979**, *14*, 415.
(56) Schäfer-Stahl, H. *Inorg. Nucl. Chem. Lett.* **1980**, *16*, 271. Schäfer-Stahl, H.; Abele, R. *Z. Anorg. Allg. Chem.*, **1980**, *465*, 147.

Mössbauer effect spectroscopy.[58] Clearly the ferrocene and related intercalates in the FeOCl host lattice provide the opportunity to examine the lattice dynamical behavior of the guest and the host species, independently, and thus probe the behavior of these anisotropic solids at two very different points in the lattice. Such studies, combined with variable (low) temperature Fourier transform infrared studies and susceptibility measurements, should add very significantly to our detailed knowledge of these fascinating materials.

Our research has been generously supported by the Division of Materials Research of the National Science Foundation, as well as by grants from the Research Council and the Center for Computer and Information Services, Rutgers University. This support is herewith very gratefully acknowledged. The author is deeply indebted to his students and co-workers, many of whom have made major contributions to the results herein discussed. In particular the contributions of Dr. Y. Maeda, Dr. A. J. Rein, T. K. McGuire, and R. Cassell have been of central importance in the pursuit of this research.

(57) Schäfer-Stahl, H.; Abele, R. *Mater. Res. Bull.*, **1980**, *15*, 1157.
(58) Schäfer-Stahl, H.; Abele, R. *Angew. Chem., Int. Ed. Engl.*, **1980**, *19*, 477. Schäfer-Stahl, H. *Mater. Res. Bull.* **1980**, *15*, 1091.

Tropomyosin: A Model Protein for Studying Coiled-Coil and α-Helix Stabilization

JAMES A. TALBOT and ROBERT S. HODGES*

Medical Research Council Group in Protein Structure and Function, Department of Biochemistry, University of Alberta, Edmonton, Alberta, Canada T6G 2H7

Received July 23, 1981 (Revised Manuscript Received March 29, 1982)

Tropomyosin is a key control protein in muscle contraction[1-3] capable of transmitting subtle conformational changes. Information in the amino acid sequence directs alignment of chains in parallel and in-register, formation and stabilization of the coiled coil, and end-to-end aggregation. In addition, the sequence provides for binding sites for actin and troponin-T and for the possible transmission of a conformational change along its length. Tropomyosin has been previously reviewed,[4,5] but we wish to discuss the requirements for the stabilization of the coiled-coil structure at the molecular level. Our comprehension of the fine control of coiled-coil stability that permits it to perform its functions depends on our understanding of the factors that are important in an α helix and a coiled coil. Work in our and other laboratories has aimed at elucidating these design principles.

Examination of X-ray crystallographic bond lengths and angles for small peptides along with the assumptions that intrachain hydrogen bonds should be maximized and linear led Pauling et al.[6] to postulate the α helix. Since then many synthetic polypeptides have been demonstrated by wide-angle X-ray diffraction to form helices with the predicted pitch of 5.4 Å per turn and with a translation along the helix axis of 1.5 Å per residue.[7]

Circular dichroism and other optical techniques have shown that single chain polypeptides are often α helical in nonaqueous solvents or at a pH far from neutrality.[8-11] Polypeptides containing a large proportion of charged amino acids, even lysine and glutamic acid copolymers where strong charge repulsion is absent, have little α helix at neutral pH when the side chains are in an aqueous environment.[12,13] Many polypeptide chains do not form helices in aqueous solutions, although they do so as part of the sequence of a globular protein molecule.[14] As a first approximation, then, α helices will not form when the side chains of the polypeptide are in an aqueous environment, since hydrogen bonds in the presence of water are exceedingly unstable.[15]

Why then do α helices exist in globular proteins like myoglobin and the highly α-helical fibrous proteins of the k–m–e–f (keratin, myosin, epidermis, fibrinogen) group of which tropomyosin is a member? In myoglobin an interior of hydrophobic side chains excludes

Robert S. Hodges was born in Saskatoon, Saskatchewan, carried out his undergraduate studies in biochemistry at the University of Saskatchewan, and received his Ph.D. degree in Biochemistry at the University of Alberta. After a postdoctoral stay in the laboratory of Dr. Bruce Merrifield at The Rockefeller University, he joined the University of Alberta in 1974. He is presently Associate Professor of Biochemistry and member of the MRC Group in Protein Structure and Function at the University of Alberta.

James A. Talbot was born in Ottawa, Ontario, and received both his B.Sc. and Ph.D. degrees in Biochemistry from the University of Alberta. He is presently in Medical School at the University of Toronto. He will be doing part-time research there with Dr. D. H. MacLennan at the Banting and Best Department of Medical Research.

(1) S. Ebashi, K. Maruyama, and M. Endo, Eds., "Muscle Contraction, Its Regulatory Mechanisms", Springer Verlag, New York, 1980.
(2) W. F. Harrington in "The Proteins", Vol. IV, 3rd ed., H. Neurath, R. L. Hill, and C.-L. Boeder, Eds., Academic Press, New York, 1979.
(3) W. D. McCubbin and C. M. Kay, *Acc. Chem. Res.*, **13**, 185 (1980).
(4) L. B. Smillie, *PAABS Revista*, **5**, 183 (1976).
(5) L. B. Smillie, *Trends Biochem. Sci.*, **4**, 151 (1979).
(6) L. Pauling, R. B. Corey, and H. R. Branson, *Proc. Natl. Acad. Sci. U.S.A.*, **37**, 205 (1951).
(7) C. H. Bamford, A. Elliot, and W. E. Hanby, "Synthetic Polypeptides", Academic Press, New York, 1956, pp 215–261.
(8) J. Applequist and P. Doty, "Polyamino Acids, Polypeptides and Proteins", M. A. Stahman, Ed., University of Wisconsin Press, Madison, WI, 1962, pp 161–175.
(9) M. Idelson and E. R. Blout, *J. Am. Chem. Soc.*, **80**, 4631 (1958).
(10) G. D. Fasman, "Polyamino Acids, Polypeptides and Proteins", M. A. Stahman, Ed., University of Wisconsin Press, Madison, WI, 1962, pp 221–224.
(11) J. T. Yang and P. Doty, *J. Am. Chem. Soc.*, **79**, 761 (1957).
(12) C. Cohen and K. C. Holmes, *J. Mol. Biol.*, **6**, 423 (1963).
(13) E. R. Blout and M. Idelson, *J. Am. Chem. Soc.*, **80**, 4909 (1958).
(14) J. A. Schellman and C. Schellman, "The Proteins", Vol. II, 2nd ed., H. Neurath, Ed., Academic Press, New York, 1964, pp 1–137.
(15) I. M. Klotz and J. S. Franzen, *J. Am. Chem. Soc.*, **82**, 5241 (1960).

0001-4842/82/0115-0224$01.25/0